

OPTICAL-PHYSICAL PROPERTIES OF NANOCRYSTALLINE STRUCTURES IN NANOPOROUS Al_2O_3 MATRICES

V. Adamiv¹, V. Horchynsky², I. Bordun², I. Teslyuk¹, R. Bukliv², A. Andrushchak²

¹Ivan Franko National University of Lviv, O.G.Vlokh Institute of Physical Optics, vol.adamiv@gmail.com

²Lviv Polytechnic National University, horchynsky@gmail.com

Variants of filling nanoporous matrices in saturated aqueous solutions are described in many publications. It has been found that ultra-small nanostructured blocks have improved mechanical, optical, magnetic and electronic properties compared to bulk substance of the same chemical composition. The works on nanoporous anodised aluminium oxide Al_2O_3 (AAO) suggest various ways of its application [1,2], taking into account the features of AAO: ordered structure, optical and physical properties, and biocompatibility. Nanoporous matrices of AAO have the following advantages: the ability to control the geometric parameters of the porous structure during their manufacture, periodicity and high porosity, and cylindrical shape of the pores. AAO can be easily dissolved without damaging the resulting nanostructures inside the pores [3]. During the filling of pores, depending on the conditions selected, partial or complete filling can be achieved, and thus nanotubes or nanorods of various shapes and sizes can be obtained [4].

Nanoporous matrices have been used to form crystal structures with predetermined physical parameters. At the same time, it is important to know what characteristics a particular matrix has. Therefore, in this study, both nanocrystal-filled AAO samples and empty starting matrices were investigated. InRedox (USA) matrices ($h = 200 \mu\text{m}$, $d = 40 \text{ nm}$) and ($h = 200 \mu\text{m}$, $d = 60 \text{ nm}$), unfilled and filled with ADP and KB5 nanocrystals, namely $\text{Al}_2\text{O}_3\text{:ADP}$ ($d = 40 \text{ nm}$) and $\text{Al}_2\text{O}_3\text{:KB5}$ ($d = 60 \text{ nm}$), were used.

The growth of ADP ($\text{NH}_4\text{H}_2\text{PO}_4$) and KB5 (KB_5O_8) nanocrystals in Al_2O_3 matrices was carried out from saturated aqueous solutions of $\text{NH}_4\text{H}_2\text{PO}_4$ and KB_5O_8 with a temperature decrease from 55 to 50°C for 1.5 hours. After that, the matrices were removed and the surfaces were cleaned of residual solution at room temperature. Before the growth, the nanoporous matrices were activated according to the procedure [5]. Subsequently, the $\text{Al}_2\text{O}_3\text{:ADP}$ and $\text{Al}_2\text{O}_3\text{:KB5}$ structures were placed in a thermostat ($\sim 60^\circ\text{C}$) for a day to evaporate excess water and finalise the formation of nanostructures [6]. X-ray diffraction studies of $\text{Al}_2\text{O}_3\text{:ADP}$ and $\text{Al}_2\text{O}_3\text{:KB5}$ confirm the formation of crystalline ADP and KB5 compounds in the pores of the matrices (Fig. 1).

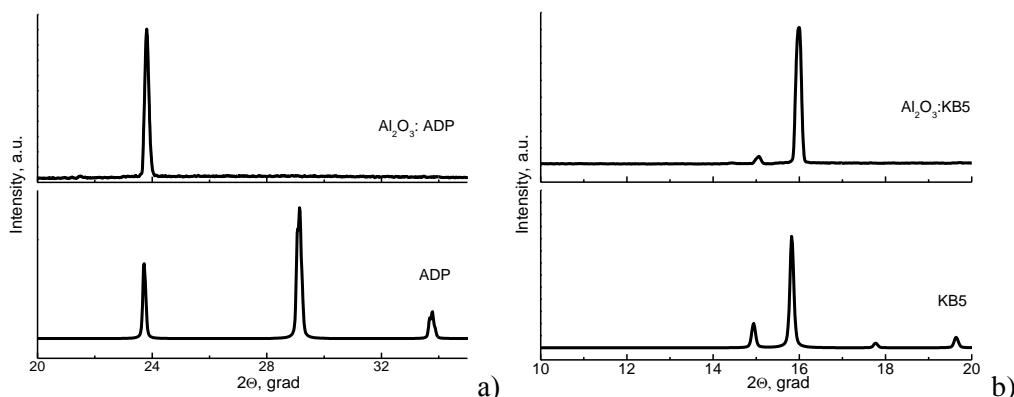


Fig. 1. X-ray diffraction patterns of nanocrystalline structures $\text{Al}_2\text{O}_3\text{:ADP}$ (a), $\text{Al}_2\text{O}_3\text{:KB5}$ (b).

Further studies of the obtained $\text{Al}_2\text{O}_3\text{:ADP}$ and $\text{Al}_2\text{O}_3\text{:KB5}$ samples and their starting Al_2O_3 matrices were carried out by scanning electron microscopy, adsorption-desorption gas porometry and visible light spectrophotometry.

Transmission spectra and surface morphology. The transmission spectra of the samples were measured in a wide spectral range (200 – 2000 nm) using a Jasco V-770 spectrophotometer. The measurement process was controlled using the Spectra Manager software. The transmission spectra of the studied samples in the visible and near-infrared regions are shown in Fig. 2. Similar dependencies were obtained by the authors of [6]. As can be seen, the $\text{Al}_2\text{O}_3\text{:ADP}$ sample absorbs the most relative to the empty matrix.

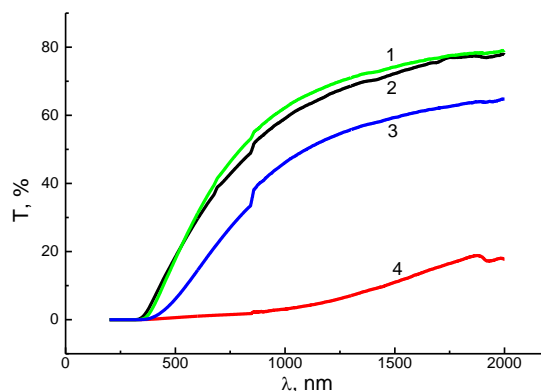


Fig. 2. Transmittance spectra of the tested AAO samples: empty matrices with pore diameters of 40 nm (1), 60 nm (2), filled matrices - KB5, 60 nm (3), ADP, 40 nm (4).

The $\text{Al}_2\text{O}_3\text{:KB5}$ sample also absorbs more than the original Al_2O_3 matrix with a diameter of 60 nm, but the difference is not so significant. The three samples have a large window of transparency in the investigated wavelength range of ~ 380 - 2000 nm (Fig. 2). The matrix filled with ADP nanocrystals has a low transmittance, so it may be promising for use as an anti-radar coating.

The morphology and pore size of the selected AAO matrices were studied using a Phenom ProX scanning electron microscope (Fig. 3). The SEM images of the matrices confirm the proportionality of the pore sizes with the dimensions specified in the original sample data and allow us to estimate the degree of pore filling with nanocrystals.

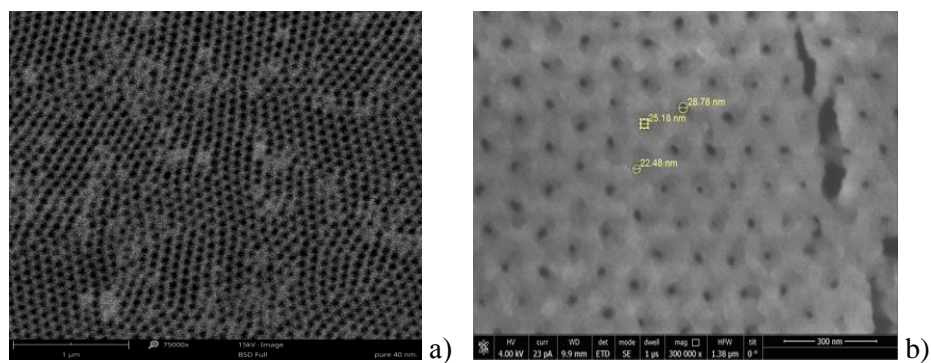


Fig. 3. SEM images of the initial (a) and filled (b) $\text{Al}_2\text{O}_3\text{:ADP}$ matrix ($d = 40$ nm)

Similar SEM images with confirmation of the morphology were obtained for Al_2O_3 ($d = 60$ nm) and $\text{Al}_2\text{O}_3\text{:KB5}$ samples. Phenom ProX, equipped with an EDS spectrometer (SDD type), is capable of performing elemental analysis of the materials under study. The surface composition was determined by surface mapping and showed the presence of only aluminium and oxygen, which confirms the high purity of the original Al_2O_3 samples.

Porometry of the studied samples. The parameters of the porous structure of the studied samples were estimated from the isothermal processes of nitrogen adsorption/desorption at its boiling point ($T = 77$ K). The adsorption/desorption isotherms were obtained using an automated analyser Quantachrome Nova

Touch LX2. Prior to measuring the isotherms, the samples were degassed in a dry helium stream at 384 K, and the degassing time was 5 hours.

When analyzing the porous structure, a certain classification of pores by size is carried out. Depending on the specific application of the porous material, this classification has additional gradations, but the classic classification remains one in which pores are divided into micropores (with a diameter of up to 2 nm), mesopores (with a diameter of 2 to 50 nm) and macropores (more than 50 nm). Since the main pores of Al_2O_3 :ADP samples are mesopores, and Al_2O_3 :KB5 samples have macropores of the lower boundary, which are close in behavior to mesopores, let us dwell on adsorption in such pores in more detail. A distinctive feature of adsorption in mesopores is the presence of capillary condensation. This phenomenon consists in the fact that condensation (volumetric filling of pores) is observed at pressures much lower than the pressure of saturated vapor above a flat liquid surface. A prerequisite for the course of capillary condensation is the presence of a film of liquid adsorbate with negative curvature on the pore walls, i.e. the liquid adsorbate must wet the pore walls. Capillary condensation can occur both reversibly and irreversibly. Irreversible capillary condensation is accompanied by hysteresis on the isotherm of adsorption/desorption of the adsorbate. The adsorption branch on the hysteresis loop will correspond to non-equilibrium thermodynamic processes. The desorption stage is equivalent to the reversible liquid-vapor transition. Therefore, it is taken for further analysis of the pore distribution or determination of the characteristics of the porous structure of samples. In reversible capillary condensation, the adsorption and desorption branches coincide.

The measured adsorption/desorption isotherms of nitrogen for the investigated samples Al_2O_3 (40 nm), Al_2O_3 (60 nm), and Al_2O_3 :ADP exhibit a characteristic hysteresis (Fig. 4), which is associated with capillary condensation of nitrogen in the pores. For the Al_2O_3 :KB5 sample, hysteresis is minimal in the region of high relative pressures (P/P_0 close to 1), while in the region of low relative pressures, the adsorption/desorption processes are well reversible. The difference in behavior between the original matrices and the matrices with crystals can be explained by the additional treatment of the matrices before crystal growth. This treatment alters the interaction parameters between the adsorbent (nitrogen) and the adsorbate (matrix with crystals).

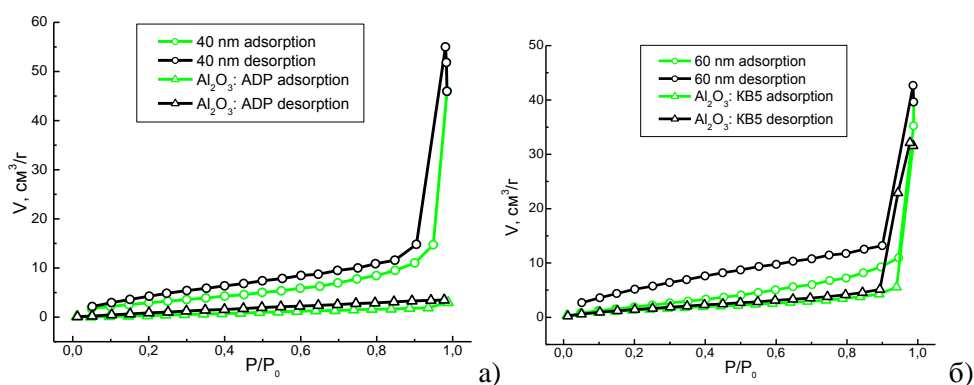


Fig. 4. Adsorption/desorption isotherms of nitrogen for the investigated samples.

To calculate the parameters of the porous structure of the materials, the obtained isotherms were analyzed using the Quantachrome TouchWin software, version 1.21. In particular, the Brunauer-Emmett-Teller (BET) multipoint method [7] was used to determine the total specific surface area, in which the experimental data are approximated by a straight line in the relative pressure range $P/P_0 = 0.05 \div 0.3$. It was found that this method is not suitable for assessing the specific surface area of Al_2O_3 :ADP samples. The correlation coefficient (the ratio between the actual and model straight lines) for this model was $R^2 = 0.4$. To use the results of the BET model, the correlation coefficient must be at least $R^2 = 0.9 \div 0.95$. For other types of samples, the correlation coefficient is quite acceptable, so the obtained results are presented in Table 1.

Since, according to the description and analysis by electron microscopy, all samples have a mesoporous structure, the classical BJH (Barret-Joyner-Halenda) method [7] was used to analyze the pore distribution of such materials. The calculation of the pore distribution was carried out by this method using the desorption isotherm, which is closer to thermodynamic equilibrium. The results obtained are given in Table. 1.

From the shape of the adsorption isotherms, the presence of a small number of micropores in the Al_2O_3 :ADP sample is most likely. The calculation of the specific surface area S_{micro} and the volume of micropores V_{micro} can be carried out by various methods. We used the Halsey t-method, which belongs to statistical methods [7]. In this method, a t-graph is constructed, which is the dependence of the volume of adsorbed gas on the thickness of the adsorption film t. The obtained results of the evaluation of the volume and specific surface area of micropores are given in Table. 1.

Table 1. Parameters of the porous structure of the studied samples

Samples	BJH		t-method		BET		$V_{\Sigma}, \text{cm}^3/\text{g}$
	$S_{\text{BJH}}, \text{m}^2/\text{g}$	$V_{\text{BJH}}, \text{cm}^3/\text{g}$	$S_t, \text{m}^2/\text{g}$	$V_t, \text{cm}^3/\text{g}$	$S_{\text{BET}}, \text{m}^2/\text{g}$	R^2	
Al_2O_3 :40 nm	12.74	0.082	0	0	11.77	0.99	0.071
Al_2O_3 :ADP	3.03	0.0045	2.93	0.00024	5.43	0.4	0.046
Al_2O_3 , 60 nm	10.1	0.06	0	0	9.89	0.994	0.062
Al_2O_3 :KB5	6.48	0.05	0	0	5.41	0.99	0.049

As can be seen from the data in Table 1, for the Al_2O_3 (60 nm) and Al_2O_3 :KB5 samples, we have very good agreement of the models with each other and with the shape of the adsorption isotherms. That is, there is no microporosity as such. The decrease in the pore content in the Al_2O_3 :KB5 sample can be attributed to the fact that part of the pores is closed by crystals. The Al_2O_3 (40 nm) matrix also has no micropores. For the Al_2O_3 :ADP sample, there is a very low micropore content, which can be attributed to the microporosity of the ADP crystals themselves. Since the ADP crystals filled the AAO matrix better than the KB5 crystals in the Al_2O_3 :KB5 sample, there are significantly fewer available mesopores in this sample.

Acknowledgements. This work was supported by the Ministry of Education and Science of Ukraine: projects Nanoelectronics (registration number 0123U101695) and Nanoarchitectonics (registration number 0124U000826).

References

1. Yaremko, O., Andrushchak, N., Adamiv V., Rosa, T., Lelonek, M., Andrushchak, A. (2019). Research of nanocomposite materials for telecommunication networks // Advanced information and communication technologies, AICT–2019: proceedings of the 3rd International conference (Lviv, Ukraine, July 2–6 2019), 96–100.
2. Atkinson, R., Hendren, W. R., Wurtz, G. A., Dickson, W., Zayats, A. V., Evans, P., & Pollard, R. J. (2006). Anisotropic optical properties of arrays of gold nanorods embedded in alumina. *Physical Review B*, 73(23), 235402.
3. Jani, A. M. M., Losic, D., & Voelcker, N. H. (2013). Nanoporous anodic aluminium oxide: Advances in surface engineering and emerging applications. *Progress in Materials Science*, 58(5), 636-704.
4. Piao, Y., Lim, H., Chang, J. Y., Lee, W. Y., & Kim, H. (2005). Nanostructured materials prepared by use of ordered porous alumina membranes. *Electrochimica Acta*, 50(15), 2997-3013.
5. Яремко О.М., Адамів В.Т., Теслюк І.М., Ольховик Б.С., Андрущак А.С., Щур Я.Й. (2020). Дослідження нанокристалітів, отриманих на основі нанопористих мембран Al_2O_3 із насичених водних розчинів KH_2PO_4 . *Наукові нотатки: Міжвузівський збірник – Луцьк: Луцький НТУ*, 70, 50-56.
6. Andrushchak N., Vynnyk D., Haiduchok V., Nikolenko A., Adamiv V., Strelchuk V., Syrotynsky O., Andrushchak A. (2023) Optical properties investigation of nanoporous Al_2O_3 matrices with embedded ADP and KB-5 crystals. Proceedings of 3rd International Conference on Innovative Materials and Nanoengineering (IMNE'2023), Dovgoluka, Ukraine. – P. 41.
7. Rouquerol, J., Rouquerol, F., Llewellyn, P., Maurin, G., Sing, K.S.W. (2014) Adsorption by powders and porous solids: principles, methodology and applications (2nd edition) Elsevier / Academic press, Oxford. – 646 pp.